

UNCLASSIFIED

Defense Technical Information Center
Compilation Part Notice

ADP011318

TITLE: Studies of Polymer-Stabilized Cholesteric Texture Films

DISTRIBUTION: Approved for public release, distribution unlimited

This paper is part of the following report:

TITLE: Display Technologies III Held in Taipei, Taiwan on 26-27 July
2000

To order the complete compilation report, use: ADA398270

The component part is provided here to allow users access to individually authored sections of proceedings, annals, symposia, etc. However, the component should be considered within the context of the overall compilation report and not as a stand-alone technical report.

The following component part numbers comprise the compilation report:

ADP011297 thru ADP011332

UNCLASSIFIED

Studies of Polymer-Stabilized Cholesteric texture films

Andy Ying-Guey Fuh^a), Chi-Yen Hung, Chi-Huang Lin, and Tsung-Chih Ko

Tainan, Taiwan 701, ROC

Department of Physics, National Cheng Kung University

ABSTRACT

We report the results obtained from the studies of polymer-stabilized cholesteric texture films. Two sets of samples were fabricated. The first set were fabricated by adding various ferroelectric liquid crystal (SmC*) dopant concentrations in the mixtures. The second were fabricated using a dual-frequency liquid crystal. The experimental results obtained from the first set show that adding a small amount of SmC* could significantly improve the cells' electro-optical (E-O) characteristics. Both the driving threshold voltage and the rise time were decreased, while the hysteresis width was increased. The result from the second set shows there exists a pronounced hysteresis effect in the transmission versus frequency curve at a given applied voltage. The hysteresis width is increasing as the applied voltage is increasing. A display mode is proposed based on this bistable feature.

Keywords : Cholesteric liquid crystal, ferroelectric liquid crystal, dual-frequency liquid crystal

1. INTRODUCTION

Liquid crystal polymer dispersions have been studied intensively owing to their fundamental importance and potential use as displays and light modulating devices.¹⁻⁹ There are basically two types of liquid crystal polymer dispersions which have been reported so far. They are polymer-dispersed liquid crystal (PDLC) and polymer-stabilized cholesteric texture (PSCT) films. The polymer concentration is usually greater than 20% in the former system to confine LC's. In addition to its use in displays and light modulating devices, it can also be used as a Gaussian filter,¹⁰ switchable gratings (both electrically¹¹ and optically¹²). The polymer concentration in PSCT films is usually below 10% for use in stabilizing the cholesteric texture LC structure in the cell. Because of its high polymer content, a PDLC film has an index-matching problem, which results in a limited view angle. This index-matching problem is eliminated in PSCT films, since the polymer concentration is low. As a result, PSCT films are haze-free at wide view angles in the clear mode, and are suitable for display applications.⁶

Depending on the surface treatment of the glass substrates and on the pitch length of the cholesteric LC, we can fabricate three types of display devices for the PSCT films. Based on the mode of operation, they are classified into normal-mode (opaque in a field-off condition and clear in a field-on condition), reverse mode (clear in a field-off condition and opaque in a field-on condition) and color-reflective bistable mode.^{6,13-14}

Usually, PSCT films are fabricated using a cholesteric LC, which is a mixture of a nematic LC and a chiral dopant. In this paper, we report the results obtained from the studies of two sets of PSCT normal-mode devices. One set was fabricated by adding various ferroelectric liquid crystal (SmC*) dopant concentrations. The other set was fabricated using a dual-frequency nematic mixed with a chiral dopant. We then measured their electro-optical (E-O) characteristics. It was found in the first set samples that adding a small amount of SmC* could improve the films' E-O characteristics significantly,

^a Author to whom correspondence should be addressed
(e-mail: andyfuh@mail.ncku.edu.tw).

such as the reduction of both the threshold driving voltage and rise-time, and the increase of the hysteresis width. The causes of such improvements were found to be due to the modification of the cells' polymer networks and the increase of fills' dielectric anisotropy with the addition of SmC* in the mixture. For the second set, there exists a pronounced hysteresis effect in the transmission versus frequency curve at a given applied voltage. The hysteresis width is increasing as the driving voltage is increasing. A display mode is proposed using a dual-frequency PSCT device based on its bistable feature of the transmission versus frequency of the driving voltage.

2. EXPERIMENTAL

Two sets of PSCT films were prepared in this experiment. The first set was fabricated as follows. The cholesteric LC used was a mixture of a nematic E48 (from E. Merck) with a chiral CB15 (E. Merck) by a weight ratio of 92.0:8.0%. A laboratory-synthesized monomer Bis[6-(acryloyloxy)hexyloxy]-1,1'-biphenylene (BAB-6) ~2.7wt% and a photoinitiator BME (~10wt% of the monomer) were then added in the cholesteric LC mixture. In a separated experiment, we have studied the dependence of this PSCT system on the monomer concentration. The result showed that the addition of ~2.7wt% of monomer gives the best E-O characteristic. The final mixture was then used to fabricate the first set PSCT cells with the addition of 0, 0.5, 1.0 and 1.5 times of SmC* (CS-2003; from Chisso) as much as CB15. In the following, we are referring these set samples as the PSCT cells having y -times SmC* in the mixture with $y=0, 0.5, 1.0$ and 1.5 .

The second set PSCT films were fabricated identically to the sample having 0-times SmC* in the first set except for the nematic in the mixture (i.e. no SmC* was added in the second set samples). In this set, the cholesteric LC used was a mixture of a dual-frequency nematic DF-02XX (Chisso) with CB15. Its dielectric anisotropy $\Delta \epsilon = \epsilon_{\parallel} - \epsilon_{\perp}$ as a function of frequency is plotted in Fig.1. Notably, $\Delta \epsilon$ is positive for $f < f_c$, and becomes negative for $f > f_c$. The crossover frequency f_c at $T=25^{\circ}\text{C}$ is ~1.1 KHz. It is also noted that no SmC* was added in the second set samples.

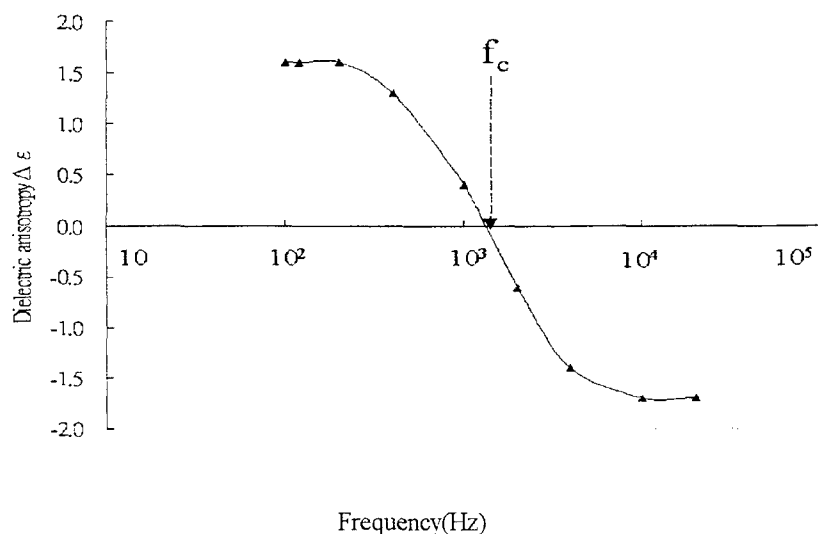


Fig. 1: Variation of the dielectric anisotropy of the dual-frequency nematic liquid crystal (DF-07XX) with respect to frequency (at room temperature). f_c is the crossover frequency.

The sample cell used in this experiment was fabricated with two indium-tin-oxide (ITO) coated glass slides, separated by a $12 \mu\text{m}$ plastic spacer. The surface of these glass substrates was cleaned without being further treated. The final mixture prepared as described above was vacuum filled into an empty cell. The filled cell was cured using a UV lamp provided by a Philips model 400/300s' metal halide lamp ~30minutes to form a sample. The UV intensity was about $3\text{mw}/\text{cm}^2$. During

curing, the LCs in a cell were aligned homeotropically with the application of a 300 Hz square-wave voltage across the ITO electrodes ($\sim 40V$, $65V$ for the first and second sets, respectively).

Details of apparatus used to perform the electro-optical measurements can be found in Ref. 15. For scanning electron microscope (SEM) study of the film's polymer network, details on how to prepare the sample can be found in Ref. 16. To measure the pitch length, cholesteric planar cells having a thickness of $12\ \mu m$ were employed using a FTIR spectroscopy. Finally, an Impedance Analyzer was used to measure the dielectric constant of LC mixtures.

3. RESULTS AND DISCUSSION

The measured E-O characteristics of the first set samples are shown in Figs. 2 and 3. Let the hysteresis width ΔV be defined as the voltage difference at the mid-point of the ramp-up curve (voltage increase) and the ramp-down curve (voltage decrease) between the maximum and minimum transmission in Fig. 2. And, the threshold (driving) voltage V_{th} is defined as the voltage of the light transmission to increase 10% from the minimum in the ramp-up curve. Notably, Fig. 2 shows that V_{th} is decreasing, but ΔV is increasing with an increasing SmC* concentration in the mixture. It is also noted from Fig. 3 that the rise-time (10-90%) and the fall-time (90-10%) are decreasing and increasing, respectively, with an increasing SmC* concentration. Based on the driving scheme designed for PSCT normal-mode displays^{6,7}, it is desired to have a lower V_{th} , but a larger ΔV .

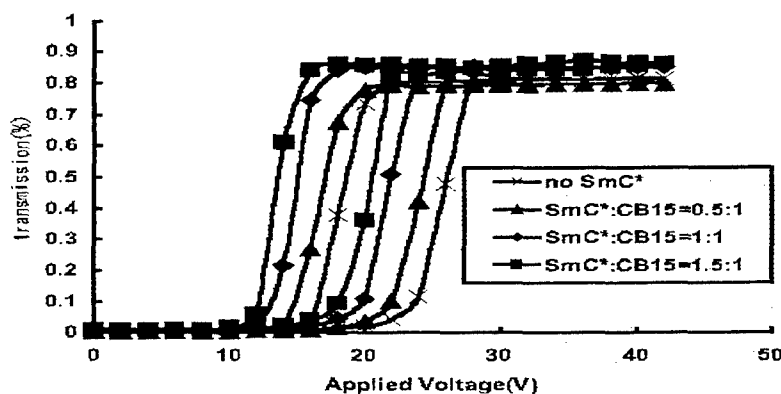


Fig. 2: Measured transmissions of the PSCT cells having y -times SmC* concentrations ($y=SmC^*/CB15$).

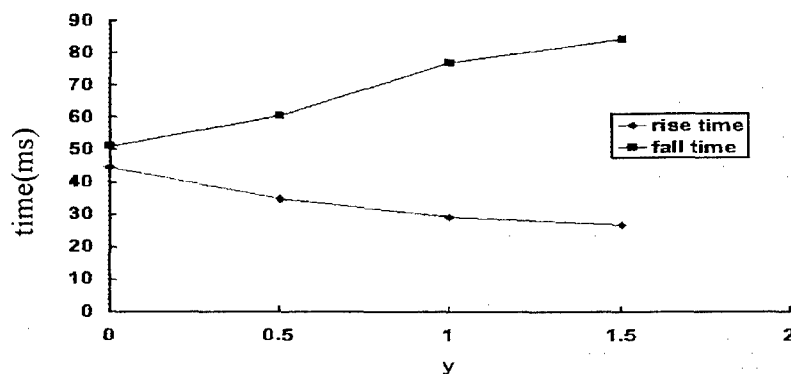


Fig. 3: The measured response times of the PSCT cells having y -times SmC* concentration ($y=SmC^*/CB15$).

In order to understand the causes that give rise to the results shown in Figs. 2 and 3. We then studied the polymer network

morphologies of these cells. The pitch length of the cholesteric LC mixtures with various SmC* concentrations was also measured. It was found that, regardless of the SmC* concentration, the cholesteric LC mixtures have about the same pitch length for the first set samples. The top-view SEM images of the cells' polymer network are depicted in Fig. 4. It is clear to see that adding a small amount of SmC* in the cell modifies the cells' polymer network morphology significantly. As the added SmC* concentration increased, more polymers were phase-separated out to form the polymer network. As a result, the formed polymer network became denser. For PSCT normal-mode cells, the polymer fibers align perpendicularly to the cells' surface. The formed polymer networks induce an alignment force on LC molecules that helps a PSCT cell to transit from its off-state (focal-conic state) to on-state (homeotropic alignment). We would expect that the denser polymer network resulting from the increasing SmC* concentration in the cell gives a stronger alignment force. The decrease of V_{th} , rise-time and the increase of ΔV and the fall-time shown in Fig. 2 and 3 are, thus, reasonable.

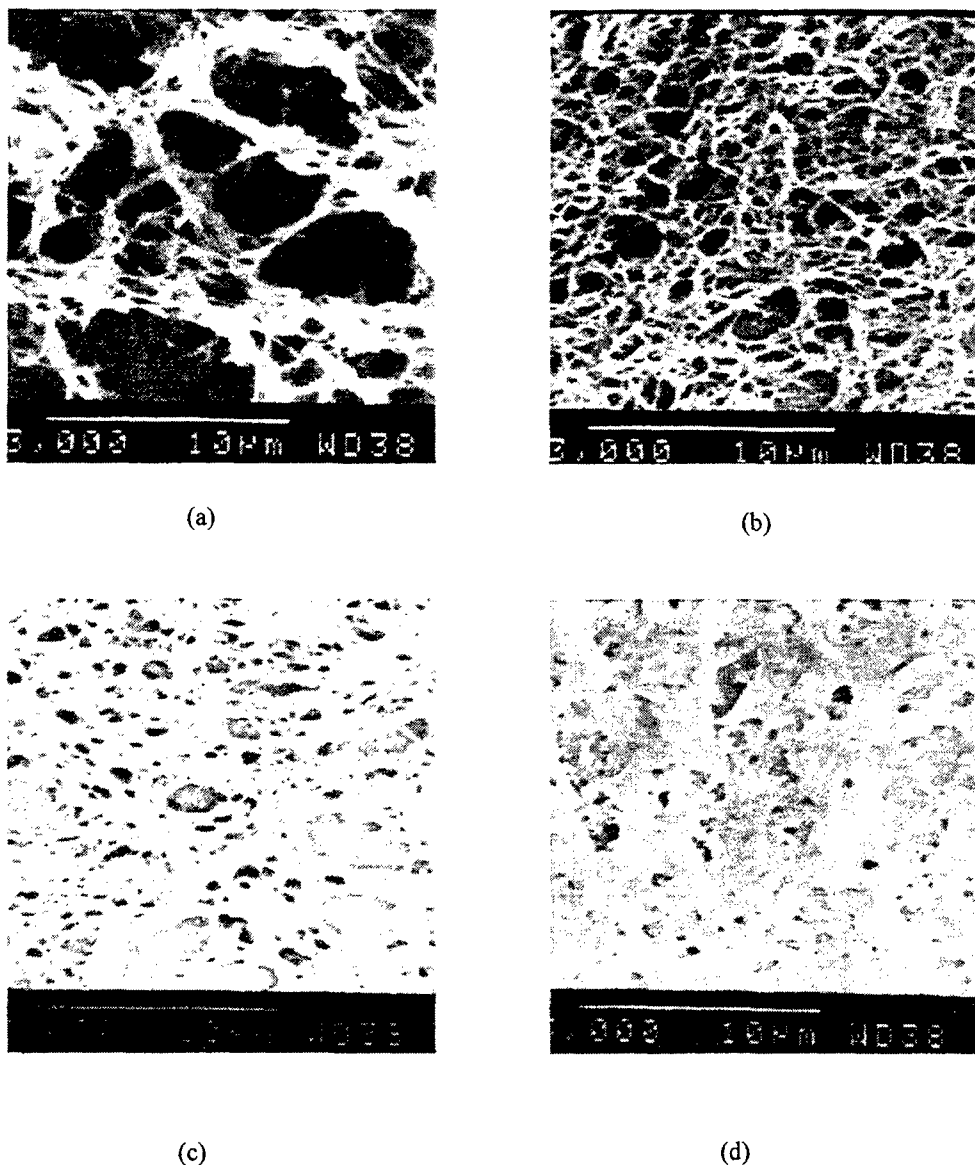


Fig. 4: Top-view SEM images of the polymer network formed in PSCT cells having y -times SmC* concentrations ($y = \text{SmC}^*/\text{CB15}$), (a) $y=0$, (b) $y=0.5$, (c) $y=1.0$, (d) $y=1.5$.

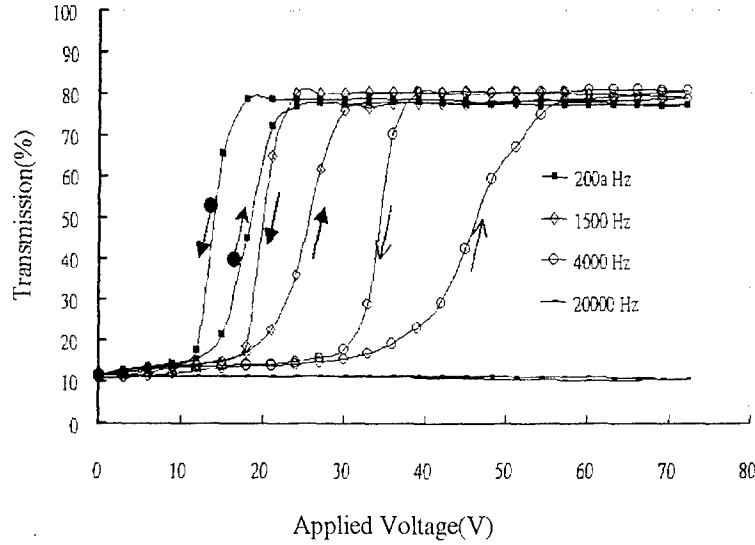


Fig. 5: Measured transmissions of a dual-frequency PSCT cell as a function of the applied voltage at four different frequencies.

Figure 5 shows the variations of the measured transmission of a dual-frequency PSCT cell with respect to the applied voltage driven at four different frequencies. Notably, both V_{th} and ΔV are increasing with an increasing frequency for the lower three frequencies. At $f=20,000$ Hz, it is not switchable. With the application of an electric field, a PSCT normal-mode cell transits from a focal-conic (helical structure) state to a homeotropic state. The V_{th} is known to be ¹⁷

$$V_{th} = \frac{2\pi d}{p} \sqrt{\frac{\pi K_{22}}{|\Delta\epsilon|}}, \quad (1)$$

where p is the pitch length, $\Delta\epsilon$ is the dielectric anisotropy, K_{22} is the twist elastic constant and d is the cell's thickness. Since $\Delta\epsilon$ of a dual-frequency LC is decreasing with an increasing frequency, for $f < f_c$, the increase of V_{th} with an increasing frequency shown in Fig. 5 is consistent with Eq. (1). At $f=20,000$ Hz, $|\Delta\epsilon|$ is believed to be very small, so the device is not switchable. It is noted from Fig. 1 that the device should be unable to be switched by an applied voltage at a frequency $f \sim f_c$. A much higher unswitchable frequency observed in Fig. 5 is believed to be due to the impurities such as CB15, BAB-6 monomer dissolved in LC. Furthermore, the decrease of ΔV with a decreasing frequency is believed to be due to the decrease of the field strength by the polarization charges. As the frequency is increasing, the liquid crystal is driven initially in the conduction regime, and then approaching to the dielectric one. The compensation effect is thus smaller as the frequency is increasing.

Figure 6 gives the variations of the measured transmissions with respect to the frequency at three driving voltages. The data points were taken every ten seconds at a given applied voltage. At low frequencies, $\Delta\epsilon$ is positive and relatively large, the cell is transparent due to its homeotropical alignment. At higher frequencies, $|\Delta\epsilon|$ becomes so small that the cell remains in the focal-conic (opaque) state. The cell transits from the homeotropical alignment (clear) to the focal-conic state (opaque) at a higher frequency when driven with a larger voltage. It is reasonable since a higher voltage could maintain the cell aligned in the homeotropical state with a relatively lower value of $|\Delta\epsilon|$ (i.e. higher frequency). It is noted from Fig. 6 that the curves trace back at different routes with lowering the frequency. There exists a pronounced "hysteresis" effect. The cause of such a "hysteresis" effect may be associated with the smaller polarization field in the higher frequency. As mentioned above, the polarization field is stronger in the low frequency (conductive) regime. The "hysteresis" width is larger when the cell is driven with a larger voltage.

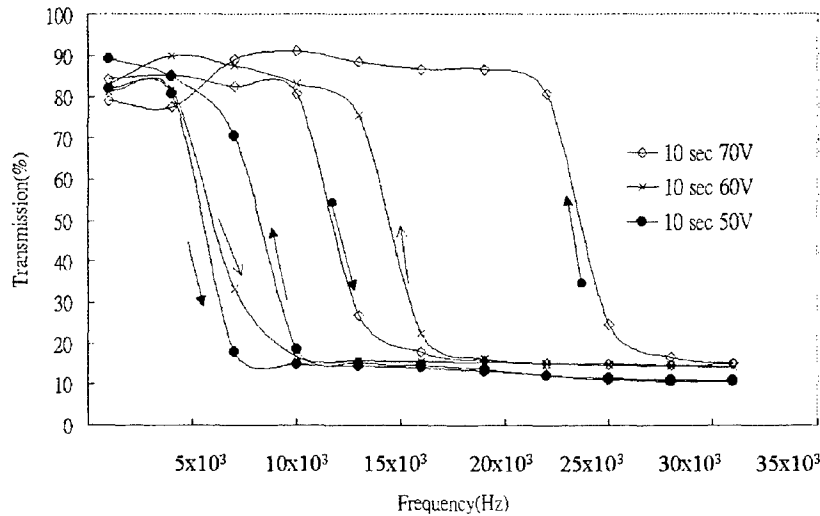


Fig. 6: Variations of the measured transmissions with respect to the frequency (T-f curve) at three driving voltages, V_{rms} = 50V, 60V and 70V. The data points were taken every ten seconds under a driven voltage

Using the bistable feature shown in Fig. 6, we propose a driving scheme for a PSCT display. Referring to Fig. 7, which is a simplified drawing representing one of curves shown in Fig. 6, the display is initially driven with an applied voltage at a frequency f_2 at C point. It is in a focal-conic (off) state. It can be switched on (homeotropical state) by increasing the frequency to f_3 ($\Delta f = f_3 - f_2$) and decreasing back to f_2 . Similarly, it can be switched off by decreasing the frequency from f_2 to f_1 ($\Delta f = f_2 - f_1$), and increasing back to f_2 .

In conclusion, we have studied two sets of PSCT samples. It is found that adding a small amount of SmC* in the mixture could result in a lower threshold voltage, a faster rise-time and a larger hysteresis width of the device. From the perspective of PSCT display applications⁷, these features are desired. In addition, a PSCT based on a dual-frequency nematic LC exhibits a pronounced "hysteresis" effect in its electrooptical curve. A display mode is proposed using this bistable feature.

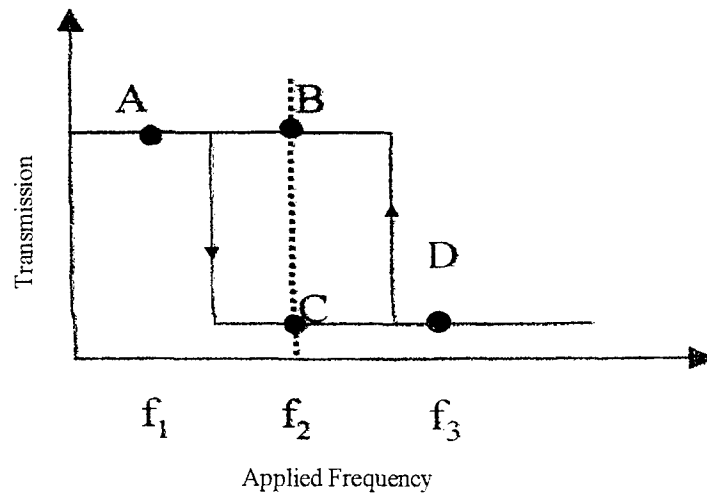


Fig. 7: A simplified T-f curve of a dual-frequency PSCT cell illustrated in Fig. 6. The cell driven by an AC voltage of frequency f_2 can be either at homeotropical (on) state or at focal-conic (off) state, depending on the change of the frequency from f_3 to f_2 or f_1 to f_2 .

ACKNOWLEDGEMENTS

The author would like to thank the National Science Council (NSC) of the Republic of China for financially supporting this research under Contract No. NSC-88-2622-E006-005.

REFERENCES

1. J. W. Fergason: SID Int. Symp. Dig. Tech. Paper **16**, (1985) 68.
2. J. W. Doane, N.A. Vaz, B. -W. Wu and S. Zumer: Appl. Phys. Lett. **48** (1986) 269.
3. P. S. Draic: J. Appl. Phys. **60** (1986) 2142.
4. S. Zumer and J. W. Doane: Phys. Rev. **A43** (1986) 3373.
5. A. Y. -G. Fuh, T. -C. Ko, Y. -N. Chyr, C. -Y. Huang, B. -W. Tzen and C. -R. Sheu: Jpn. J. Appl. Phys. **32** (1993) 3526.
6. D. -K. Yang, L. -C. Chien and J. W. Doane: Appl. Phys. Lett. **60** (1992) 3102.
7. A. Y. -G. Fuh, C. -Y. Huang, M. -S. Tsai and G.-L. Lin: Chin. J. Phys. **33** (1995) 291.
8. J. W. Doane, D. -K. Yang and Z. Yaniv: Proc. SID, Japan Display 1992, p-73.
9. Y. Fung, D. -K. Yang, J. W. Doane and Z. Yaniv: Research conf. Euro Display 1993, p-157.
10. A. Y. -G. Fuh, C. -Y. Huang, B. -W. Tzen: Jpn. J. Appl. Phys., part1 **33** (1994) 1088.
11. A. Y. -G. Fuh, M. -S. Tsai, C. -Y. Huang, T. -C. Ko, and L.-C. Chien: Opt. Quantum Electron **28** (1996) 1535.
12. A. Y. -G. Fuh, M. -S. Tsai, L. -J. Huang and T. -C. Liu: Appl. Phys. Lett. **74** (1999) 2572.
13. D. -K. Yang, L. -C. Chien, and J. W. Doane: SID 1991 Int. Symp. Dig. (1991) p.49.
14. D. -K. Yang, L. -C. Chien and J. W. Doane: SID 1992 Int. Symp Dig. (1992) 759.
15. A. Y. -G. Fuh, T. -C. Ko and M. -H. Li: Jpn. J. Appl. Phys. **31** (1992) 3366.
16. A. Y. -G. Fuh, C. -Y. Huang and C. -W. Lau: Jpn. J. Appl. Phys. **36** (1997) 2754.
17. P. G. deGennes: Solid State Comm. **6** (1968) 168..